Formal Behaviour Classification under Uncertainty

Applying Formal Analysis to System Dynamics

Jurgen Kuipers
Delft University of Technology
jurgen.kuipers@gmail.com

A study was performed by the author on formal analysis of uncertain non-linear systems in the context of System Dynamics (SD). The objective of this study was to develop a more insightful method to classify model behaviour for exploratory modelling. The long term vision of this study is more efficient, more exhaustive and more insightful model behaviour exploration than the current sampling and clustering approaches. To illustrate the possibilities this, a simple predator-prey model from literature was analysed. Uncertainties were specified on the parameters and the resulting behaviour was represented in phase portraits. Through further analysis of local, linearised behaviour around equilibrium points, classes of behaviour were defined on mathematical properties of the system instead of properties of the output. For the predator-prey model, these behaviour classed resulted in well-defined boundaries in the uncertainty space. The major finding of the study is that formal analysis can analytically split the uncertainty space into sub-spaces that result in different behaviour, thereby offers an alternative to the current behaviour classification methods.

1 Introduction

This paper treats formal analysis of uncertain non-linear systems, in the context of System Dynamics (SD). The systems considered in SD are often prone to uncertainty caused by difficult or impossible identification of the system equations. Therefore, exploratory modelling is chosen over predictive modelling. Currently, this is done in the Exploratory System Dynamics Modelling and Analysis (ESDMA) approach [1, 2], based on the work of Bankes in 1993 [3]. Here, all uncertainties are identified and the influence of these uncertainties is investigated, often through a large number of simulations. Analysis and clustering of thousands of runs follows, which sometimes requires some tinkering and is computationally expensive. Also, this hardly ever leads to a clear and insightful result.

Formal analysis is presented as an alternative to the numerous simulations that post-processed and interpreted. Formal analysis allows one to define criteria on the outputs of a model up front, and consequently search for which uncertainties these hold or do not hold. This allows for more and different insight into the impact of uncertainty on a model. As an example, a simple predator-prey model with deeply uncertain parameters is introduced, and analysed. The methodology is further elaborated on and the possible future developments are sketched. A more mathematical treatment of the method and this particular example can be found in [4].

2 Example Predator-Prey System

2.1 The Predator-Prey Model

Assume given the predator-prey model in Figure 1, which is adapted from Bossel [5, p. 105-109]. The goal of the model is to describe the population development over time. Figure 1 is the proper model, according to SD standards.

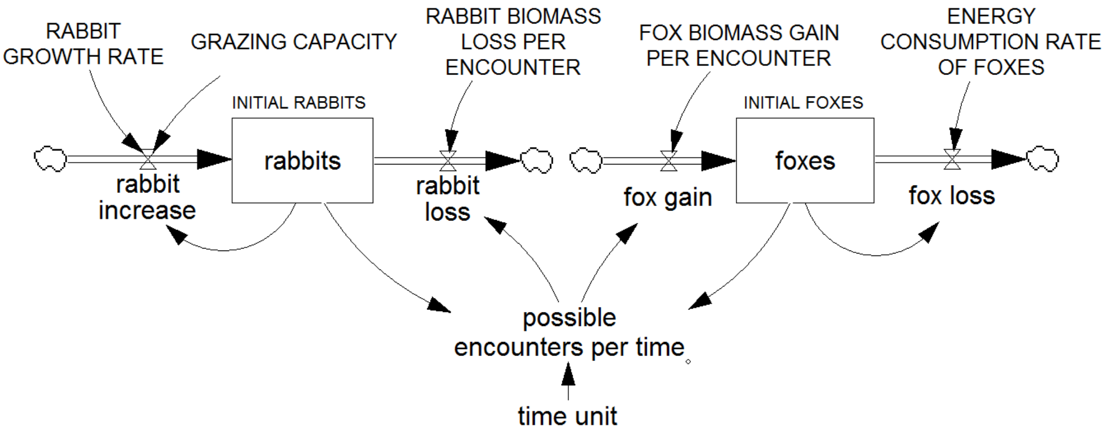

Figure 1: Stock-flow model of the predator prey example Eq. (??), adapted from [5, p. 105-109]

The parameters and initial condition are easily found in the stock-flow diagram; they only go into the model and are not affected by it. Therefore, they are at the back end of the arrows. Also, all constants and initial state values are written in capitals.

The model in Figure 1 is characterized by a prey population x_1 and a prey population x_2, isolated from other species. Under the assumption that the prey is herbivorous and grazing capacity is unlimited, the following exponential growth and decay are recognized:

$$\dot{x}_1 = ax_1 \tag{1a}$$
$$\dot{x}_2 = -dx_2 \tag{1b}$$

with x_1 the prey population in prey biomass units (for example number of rabbits) and x_2 the predator population in predator biomass units (for example number of foxes). Eq. (1) assumes the following:

1. The prey always have ample food available
2. The rate of change of a population is proportional to its size
3. The environment is considered to be constant and no evolution or adaptation occurs
4. The predators die due to age

The growth rate a is a positive constant that defines the exponential growth of the prey. The predators in Eq. (1b) have no food, and undergo exponential decay, according to the energy consumption rate d.

The predator and prey have encounters in the middle of Figure 1, and they exchange biomass. The interaction between the populations is modelled with three more assumptions:

5. The actual encounters are proportional to the total number of combinations of a predator and a prey ($x_1 x_2$)
6. The food supply of the predators consists only of the prey population
7. Predators are always hungry

Thus, the possible encounters per time scale with $x_1 x_2$. When prey meets a predator, with a certain probability, the prey is killed and eaten. The average biomass lost from the prey per possible encounter is defined as b, and the biomass increase of the predator is c. Both b and c are positive constants. The resulting differential equation, together with initial conditions $x_1(0) = x_{1,0}$ and $x_2(0) = x_{2,0}$, is

$$\dot{x}_1 = a x_1 - b x_1 x_2 \tag{2a}$$
$$\dot{x}_2 = c x_1 x_2 - d x_2 \tag{2b}$$

From Eq. (2) it is readily observed that b and c are weights of non-linear coupling terms. Also, there are no inputs acting on the system. This means that Eq. (2) is an autonomous, non-linear set of differential equations.

The last step in describing the model in Figure 1, is imposing a grazing capacity limit for the prey. For demonstrative purposes, it is assumed that there is a maximum size of the prey population that can be supported by the environment. This is called the grazing capacity $x_{1,\text{cap}}$ and removes the first assumption. The effect of the grazing capacity on the prey increase can be modelled with a simple logistic function [5]. Expanding Eq. (2) with this restriction results in:

$$\dot{x}_1 = a x_1 \left(1 - \frac{x_1}{x_{1,\text{cap}}}\right) - b x_1 x_2 \tag{3a}$$
$$\dot{x}_2 = c x_1 x_2 - d x_2 \tag{3b}$$

This results in a differential equation with two states and five parameters, which keeps the model simple enough to analyse analytically. Bossel published a base set of parameters $\theta := [a, b, c, d, x_{1,\text{cap}}]^T$ and initial values $x_0 := [x_{1,0}, x_{2,0}]^T$[5, p. 109]. This can be seen in Table 1.

Table 1: Parameters and initial values for the predator-prey example, from Bossel [5, p. 109]

Parameter		Base	Units
rabbit growth rate	a	0.08	1/week
rabbit biomass loss per encounter	b	0.002	$\frac{\text{rabbit biomass}}{\text{rabbit biomass*fox biomass}}$
fox biomass gain per encounter	c	0.0004	$\frac{\text{fox biomass}}{\text{fox biomass*rabbit biomass}}$
energy consumption rate of foxes	d	0.2	1/week
grazing capacity	$x_{1,\mathrm{cap}}$	1000	rabbit biomass
initial rabbits	$x_{1,0}$	500	rabbit biomass
initial foxes	$x_{2,0}$	10	fox biomass

2.2 Base Case Results

The results of the predator prey model with a limited grazing capacity are compared to the case where the grazing capacity is unlimited. The latter case is approximated by setting $x_{1,\mathrm{cap}} = 10^8 \gg x_1$. The behaviour of the system over time is displayed for the first 250 weeks ($\approx$ 5 years) in Figure **??**.

Figure 2a shows the model with grazing capacity $x_{1,\mathrm{cap}} = 10^8$, to simulate unlimited grazing. This is the typical oscillation present in unconstrained Lotka-Volterra or predator-prey systems. At $t = 0$, there are only a few predators; not a lot of prey are killed and prey growth is observed. This increase in prey is followed by an increase in predators. This is explained by larger availability of food due to the growth of the prey population. Because of the fact that the predators also started to grow, the encounters and thus killings increase. This causes the prey population to decrease rapidly. After a while the predator population follows the decrease, because of the decrease in their food source. That in turn, gives ample possibility for the prey to start growing again, and the cycle starts over.

In Figure 2b, the size of the populations over time can be seen for the limited grazing capacity of $x_{1,\mathrm{cap}} = 1000$. The grazing limitation results in damping of the oscillations. The predator population still has a lag compared to the prey, and the oscillation seems to be a little bit slower than before.

When both these runs are plotted in the $x_1 - x_2$ phase plane in Figure 3, the oscillatory behaviour translates into clockwise spirals. The predator lag is still apparent. Note that the run with restricted grazing branches off of the run with unrestricted grazing, and converges to a stationary point; a different point than the equilibrium that the unrestricted model is circling around. The unrestricted grazing, where $x_{1,\mathrm{cap}} = 10^8$, seems to trace the same loop. It is unclear whether it does, or if it converges or diverges very slowly. Either way, the influence of a single parameter is very apparent. The explanation of the behaviour in Figure 3 and the influence of different parameters are further treated in Section **??** and Section **??**.

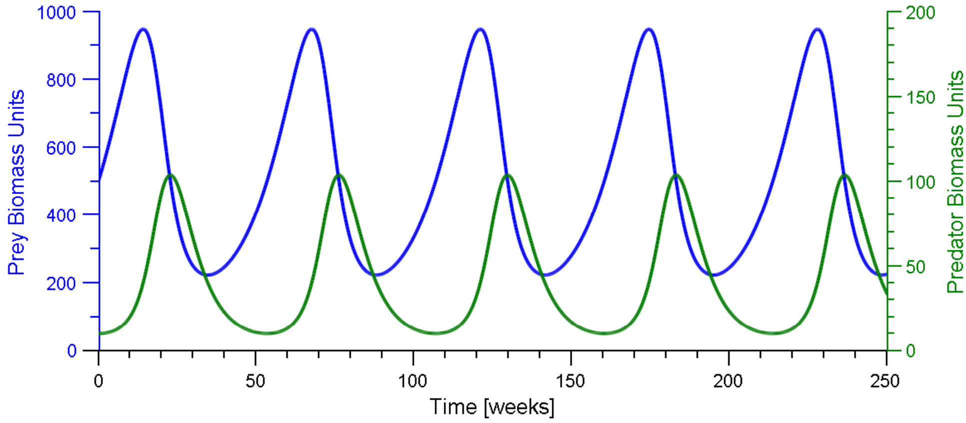

(a) Without grazing capacity, $x_{1,\text{cap}} = 10^8 \gg x_1(t)$

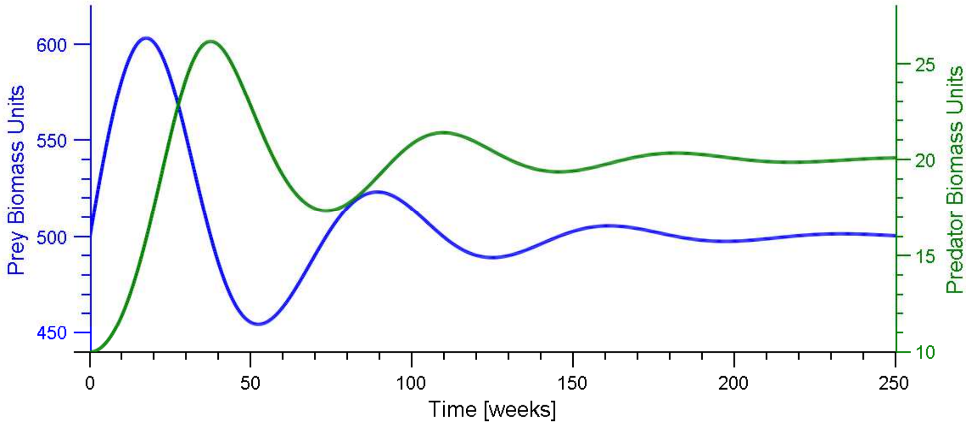

(b) With grazing capacity, $x_{1,\text{cap}} = 1000$

Figure 2: Results of the predator prey model Eq. (**??**), with $\theta = \theta_{\text{base}}$. Prey in blue on the left axes and predator in green on the right.

3 Uncertainty

Uncertainty is often present in System Dynamics models due to the nature of the social-technical issues that are considered. Parameters are hard to identify or not measurable at all, it is very difficult to measure social-technical systems accurately, and different views of the world lead to different models of the same system. The inclusion of as many uncertainties as possible is important, as it allows for more robust decision making by including more possible scenarios.

In this paper, the main focus lies on input uncertainty, because of the more insightful procedure of analysis. Pruyt considers inputs to be all the input the model uses [6]. As SD models are to a high extent endogenous (causally closed) [7, p. 38],[8, 9], inputs consists mostly of parameters and initial conditions.

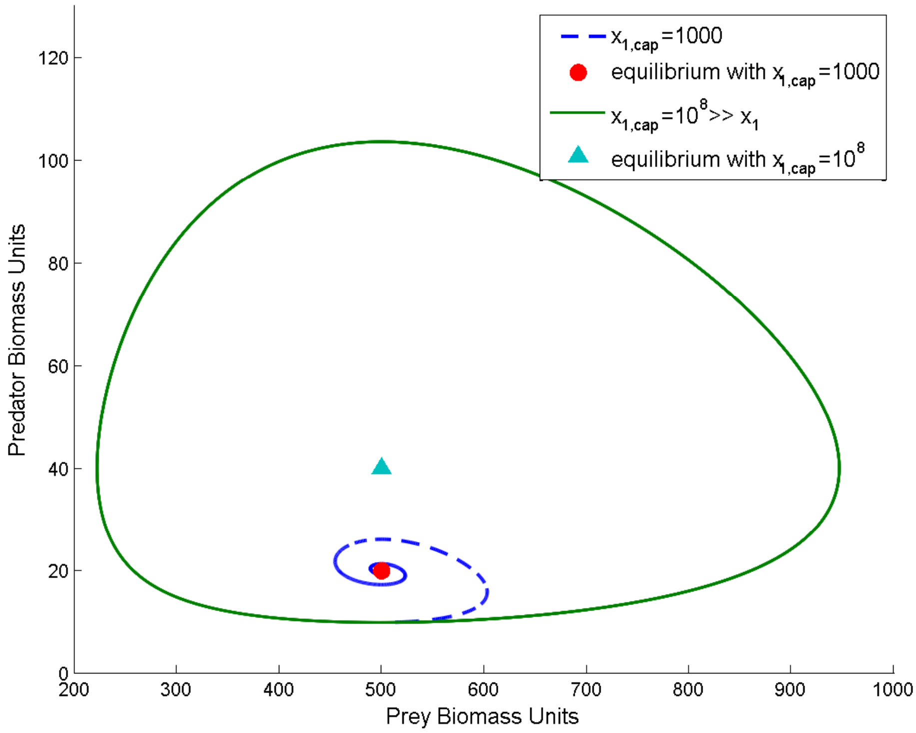

Figure 3: Results of the predator prey model Eq. (??), with $\theta = \theta^1$ in the $x_1 - x_2$ plane. Compare with and without grazing capacity for the prey.

3.1 Input Uncertainties in the Model

Recall the predator-prey model from Eq. (3) with the base case defined in Table 1. As the predator-prey model is just an example, it is assumed that no measured data is available and the exact values for the parameters $\theta := [a, b, c, d, x_{1,\text{cap}}]^T$ and initial state $x_0 := [x_{1,0}, x_{2,0}]^T$ are uncertain. In order to get a grip on the uncertainty, the ranges on the parameters are determined in Table 2 to create the uncertainty space; the combination of all these ranges. With five variables for the parameters and two for the initial condition, there is a total of seven uncertainties, with each range at least an order of magnitude.

4 Exploratory System Dynamics Modelling and Analysis

When acknowledging deep uncertainty, one quickly ends up with a large set of possible combinations of uncertainties, as in Table 2. To adequately treat the set of models resulting from the combinations of uncertainties, Steve Bankes initiated the move from predictive

Table 2: Parameters, base case values and their uncertainty ranges

Parameter		Base	Range	Units
rabbit growth rate	a	0.08	$[0.02, 0.5]$	1/week
rabbit biomass loss per encounter	b	0.002	$[0.001, 0.01]$	$\frac{\text{rabbit biomass}}{\text{rabbit biomass*fox biomass}}$
fox biomass gain per encounter	c	0.0004	$[0.0001, 0.002]$	$\frac{\text{fox biomass}}{\text{fox biomass*rabbit biomass}}$
energy consumption rate of foxes	d	0.2	$[0.05, 0.5]$	1/week
grazing capacity	$x_{1,\text{cap}}$	1000	$[100, 1000]$	rabbit biomass
initial rabbits	$x_{1,0}$	500	$[10, 750]$	rabbit biomass
initial foxes	$x_{2,0}$	10	$[1, 40]$	fox biomass

modelling towards exploratory modelling in 1993 [3]. Nowadays, the field Bankes initiated is called Exploratory Modelling and Analysis (EMA), or ESDMA when applied to SD.

4.1 Random Sampling of the Uncertainty Space

To illustrate the impact that uncertain parameters have on a model, the example of the predator-prey model is analysed. With the uncertain ranges and constraints stated in Table 2, 100 parameter sets and initial conditions were randomly chosen from the uncertainty ranges, with which the model was run. This serves just as a demonstration, but from the results in Figure 4 it can be seen that interpreting the outputs is no trivial matter. From Figure 4a it can be seen that oscillations with different time period are present, some runs are converging within 50 weeks, while others hardly seem to converge at all.

Overall, it is clear that further analysis of the outcomes is required. Many authors use numerical sensitivity analysis to changes in uncertain parameters around a base case, by applying small changes to the parameters and sketching the envelop of outcomes[2, 10, 11, 12, 13]. Kwakkel and Pruyt list the PRIM and Classification and Regression Trees as two rule inducing methods. Yücel and Barlas [13] and Kwakkel *et al.* [14] use time series clustering algorithms.

Formal analysis offers an alternative to previously mentioned methods. Furthermore, no sampling is required as no model runs are performed. This analysis separately treats uncertainty on the initial values and uncertainty on the parameters.

4.2 Uncertainty on the Initial Values

Uncertainty on the initial values can most easily be depicted in the $x_1 - x_2$ plane. Because time is not explicitly present in those plots, multiple outputs can easily be plotted onto the same graph without becoming a mess. Each pair of outcomes $x_1(t)$ and $x_2(t)$ is represented

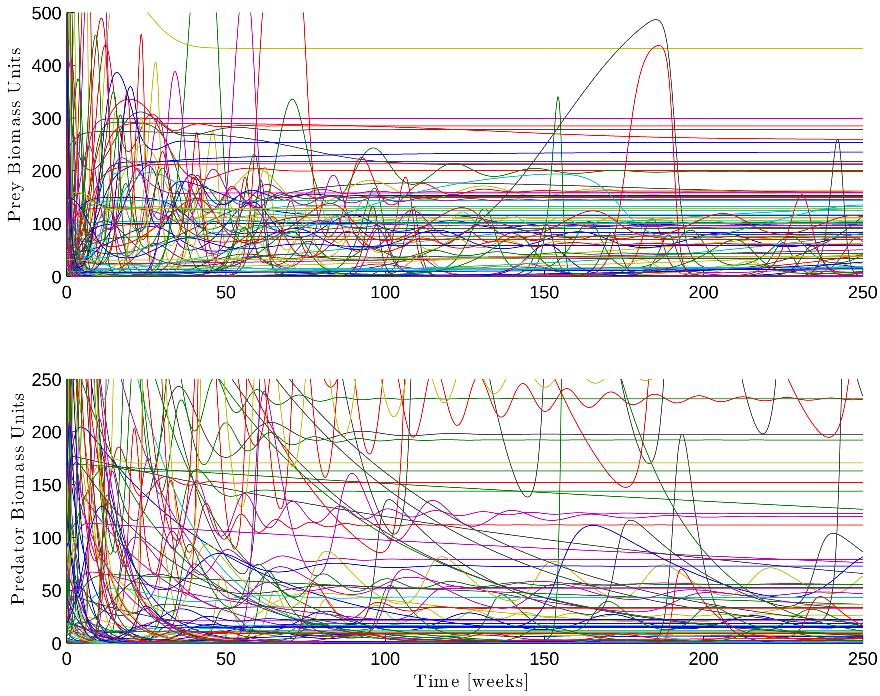

(a) Prey and predators over time, for the randomized parameter set, zoomed in to increase readability

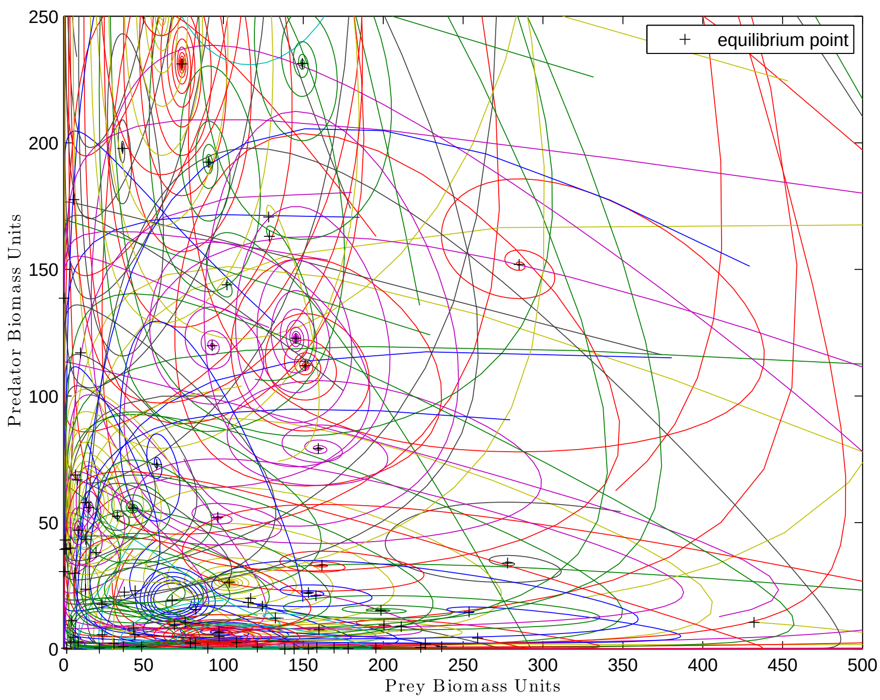

(b) Prey and predators plotted against each other, zoomed in to increase readability

Figure 4: Exploring uncertainty: 100 runs randomly sampled in the uncertainty space as defined in Table 2. Made with Matlab.

as a curved arrow, and the system follows the arrow in forward direction as time progresses. If the initial values are chosen carefully, they sketch the family of solutions for all initial values for a fixed parameter set. The family of all solutions to a model with all possible initial values is called a phase portrait. In practice, only a couple of solutions are drawn. Examples of phase portraits for the predator-prey model are shown in Figure 5. For further information on phase portraits, see Appendix A.

In Figure 5a, several curves enter from the upper-right. The prey population decreases as the predators increase until they reach a maximum. The predators decrease after that, until the prey population reaches a minimum. They spiral towards an equilibrium point that has 500 prey and 20 predators. In the base case, all the oscillatory behaviour that spirals toward this equilibrium point is considered to be similar. Figure 5b shows a set of closed loops for positive numbers of predators and prey. The equilibrium point where these loops circle around is at 500 prey and 40 predators. These loops are all considered to be similar behaviour.

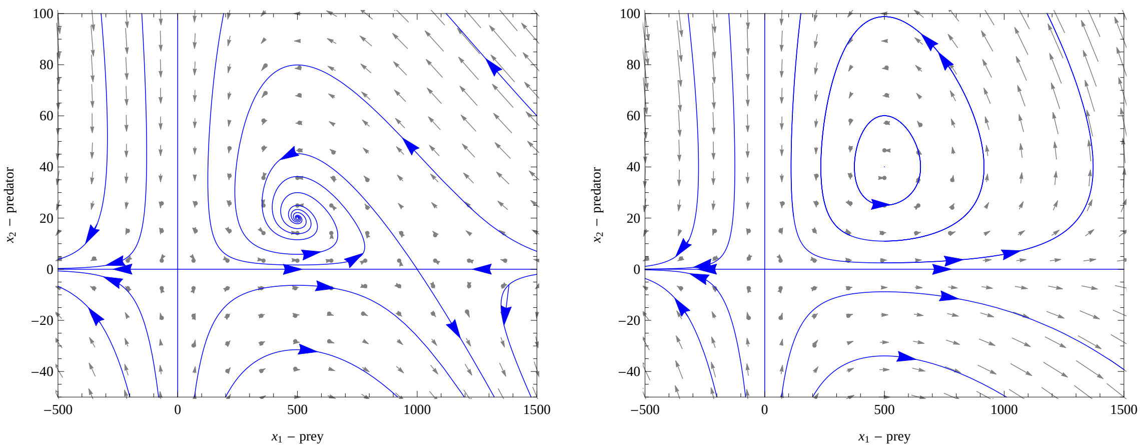

(a) Base parameter set, $x_{1,\mathsf{cap}} = 1000$ **(b)** Base parameter set with $x_{1,\mathsf{cap}} = 10^8$

Figure 5: Phase portrait consisting of multiple ouputs (in blue) in the $x_1 - x_2$ plane of the predator-prey system in Eq. (3). The light grey arrows represent the local direction that the outputs follow. Made with CurvesGraphics6.

Now that it is known that phase portraits in the $x_1 - x_2$ plane contain a considerable amount of information about a model for all initial conditions, the question might arise how much these phase portrait will vary with changing, uncertain parameters. In Figure 5 it is readily observed that changing the grazing capacity for prey $x_{1,\text{cap}}$ from 1000 to 10^8 changes the phase portrait considerably. More of these changes can be found through formal analysis of the parameter uncertainty in Section 5.

5 Formal Analysis under Parameter Uncertainty

By varying the grazing capacity for prey alone, several completely different phase portraits are found for the predator-prey model. If the assumption that the prey population x_1 is always lower than the grazing capacity for prey $x_{1,\text{cap}}$ is released, a third and fourth case can be added to the previously considered phase portraits in Figure 5. This can be thought of as an effect of deforestation for example, where the plants suddenly get removed and the grazing capacity for prey drops lower than the prey population. The resulting four phase portraits are shown in Figure 6. In order to perform insightful classification of behaviour, a criterion is needed to decide whether two phase portraits are in the same behavioural class or not. If phase plots differ only slightly, and show similar overall behaviour, they are in the same class. As long as there is a spiral located between and above two saddle points, this means that the behaviour is considered similar to that of the base case in Figure 5a.

In order to compare the phase portraits in Figure 6 and to systematically search for topologically different phase portraits, an analytical framework is introduced in the remainder of this section.

One of the analytic tools is the separatrix, displayed as bold red lines in Figure 6. They are special solutions leading to and from equilibrium points that split the state space in two. See Appendix B for a detailed description of separatrices.

5.1 Local Behaviour

To get a better understanding of phase portraits, it is useful to first look at each equilibrium points separately. Khalil [15] states tbat local behaviour around an equilibrium point $\bar{x}$ of a non-linear differential equation is based on the eigenvalues of the linearisation. Consider the predator-prey system Eq. (3):

$$\dot{x}_1 = ax_1\left(1 - \frac{x_1}{x_{1,\text{cap}}}\right) - bx_1x_2 \tag{4a}$$

$$\dot{x}_2 = cx_1x_2 - dx_2 \tag{4b}$$

with parameters $a, b, c, d, x_{1,\text{cap}} > 0$ and initial state $x_{1,0}, x_{2,0}$.

With $x = [\text{prey}, \ \text{predator}]^T$, three equilibrium points can be found by setting $\dot{x} = 0$

$$\bar{x}_1 = \begin{bmatrix} 0 \\ 0 \end{bmatrix}, \qquad \bar{x}_2 = \begin{bmatrix} x_{1,\text{cap}} \\ 0 \end{bmatrix}, \qquad \bar{x}_3 = \begin{bmatrix} \frac{d}{c} \\ \frac{a(-d+cx_{1,\text{cap}})}{bcx_{1,\text{cap}}} \end{bmatrix} \tag{5}$$

From these analytic expression, it is clear that the positions of the equilibrium point change with the parameters. The first equilibrium, $\bar{x}_1$ is the state of total extinction; no predators nor prey are alive. In $\bar{x}_2$, the predators went extinct, but the prey survived to grow until restricted by the grazing limit, $x_{1,\text{cap}}$. Both the first, as well as the second equilibrium

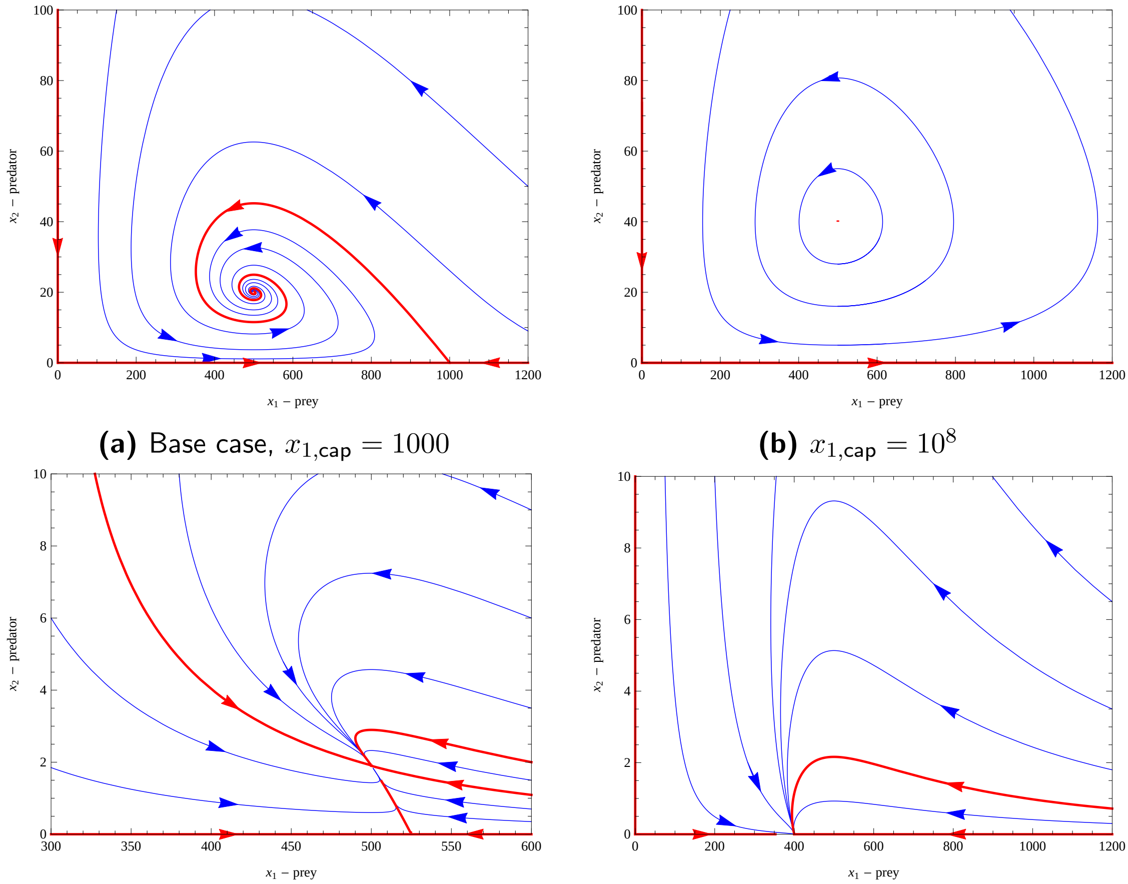

(a) Base case, $x_{1,\mathsf{cap}} = 1000$ **(b)** $x_{1,\mathsf{cap}} = 10^8$

(c) $x_{1,\mathsf{cap}} = 525$, zoomed in **(d)** $x_{1,\mathsf{cap}} = 400$, zoomed in

Figure 6: Phase portrait (in blue) of the predator-prey system for the base case, where $x_{1,\mathsf{cap}}$ is varied. The separatrices that split up the plane into regions of behaviour are in bold red. Made with CurvesGraphics6. See Appendix B for a detailed description on separatrices.

are not too hard to imagine, but the third equilibrium is the interesting one. All the parameters in $a, b, c, d, x_{1,\mathsf{cap}}$ are present.

With the base parameters as defined in Table 1, these equilibrium points become:

$$\bar{x}_1 = \begin{bmatrix} 0 \\ 0 \end{bmatrix}, \qquad \bar{x}_2 = \begin{bmatrix} 1000 \\ 0 \end{bmatrix}, \qquad \bar{x}_3 = \begin{bmatrix} 500 \\ 20 \end{bmatrix}$$

These points can be found as either begin or end points of the bold red separatrices in Figure 6a. To analyse local behaviour, linearisations around these equilibrium points are made:

$$\dot{x} = Ax, \quad \text{with} \quad A \stackrel{\text{def}}{=} \left.\frac{\partial \dot{x}}{\partial x}\right|_{x_{eq}} \tag{6}$$

For the first equilibrium point, it can be found from Eq. (3) that the linearisation has eigenvalues $\lambda_1 = -0.2$ and $\lambda_2 = 0.08$. Solely based on the sign and value of the eigenvalues of the linearization, a classification of the local behaviour can be made [15, Chapter 2]. This means that $\bar{x} = [0,\ 0]^T$ is a saddle.

Similarly, the second equilibrium point, $\bar{x}_2 = [1000,\ 0]^T$, has $\lambda_1 = -0.08$ and $\lambda_2 = 0.2$, which is also a saddle point. The thirds equilibrium point at $\bar{x}_3 = [500,\ 20]^T$ is stable focus, because of the complex eigenvalues $\lambda_{1,2} = -0.02 \pm 0.0872\imath$ with a negative real part.

With this knowledge, the next step is to visualize the neighbourhoods of these equilibrium points. Their local phase portraits are depicted in Figure 7. Combining these local phase portraits with the location of the equilibrium points, one can see the resemblance with the phase portrait of the non-linear system in Figure 6 quite easily.

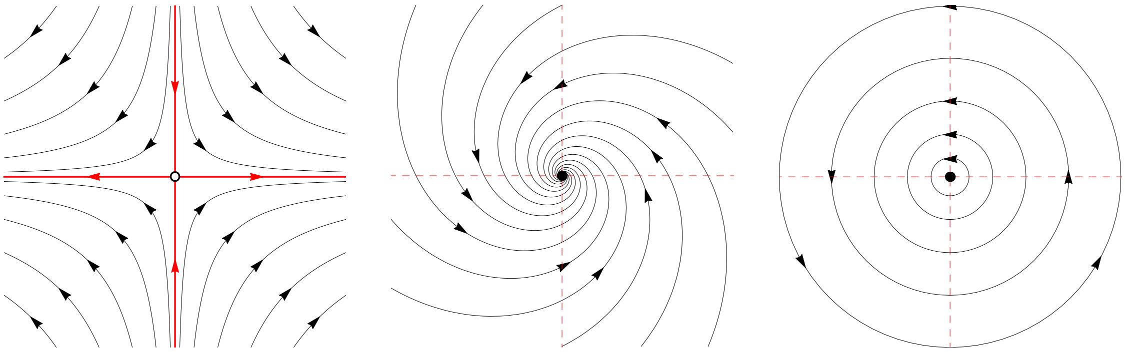

(a) Saddle, $\bar{x}_1$ and $\bar{x}_2$ for all cases

(b) Stable focus, $\bar{x}_3$, base case, $x_{1,\text{cap}} = 1000$

(c) Centre, $\bar{x}_3$, suspected for $x_{1,\text{cap}} = 10^8$

Figure 7: Phase portrait (in black) of the local, linearised behaviour around the equilibrium points. The separatrices are in bold red. Made with CurvesGraphics6.

The third equilibrium point seems to have changed to a centre for $x_{1,\text{cap}} = 10^8$ in Figure 6b. At what value of $x_{1,\text{cap}}$ does this change occur? Another change is that in the comparison between Figure 6a and Figure 6c, an equilibrium point seems to have disappeared. Again, only $x_{1,\text{cap}}$ is varied. For what value of $x_{1,\text{cap}}$ does an equilibrium point disappear, and what happens close to that value? These changes are considered bifurcations, and are treated next.

5.2 Bifurcations

Khalil defines bifurcations as "a change in the equilibrium points or periodic orbits, or their stability properties, as a parameter is varied" [15, p. 70]. That means that bifurcations can be seen as the boundaries of behaviour classes. Many well known bifurcations are described in literature [15, 16, 17].

Recall that in Eq. (5) the three equilibrium points are stated as function of the parameters. In the case of the base parameters, these equilibrium points are unique. However, for grazing capacity $x_{1,\text{cap}} = d/c = 500$ it is found that $\bar{x}_2 = \bar{x}_3$. For $x_{1,\text{cap}} > d/c = 500$, the position of $\bar{x}_3$ is under the x_1-axis. This can be seen in Figure 6d. The system now has two equilibrium points:

$$\bar{x}_1 = \begin{bmatrix} 0 \\ 0 \end{bmatrix}, \qquad \bar{x}_2 = \begin{bmatrix} x_{1,\mathrm{cap}} > 500 \\ 0 \end{bmatrix},$$

The first equilibrium point, and its linearisation remain unchanged. The linearisation around $\bar{x}_2$ now has eigenvalues $\lambda_1 < 0$ and $\lambda_2 < 0$. That means that the equilibrium point is a stable node that is approached from all sides. When looking at the phase portrait with separatrices in Figure 6d, the position of the equilibrium point at the x_1-axis, absence of the oscillations, and the shifting of the separatrix of $\bar{x}_2$ are readily observed.

To find the case of Figure 6c, the eigenvalues have to be checked analytically for changes in signs and from complex to real-valued. The tipping point between the complex eigenvalues of $\bar{x}_3$ in the spiral and real eigenvalues is found to be at exactly $50(5+\sqrt{35}) \approx 545.804$. That means that a new scenario has been found where $500 < x_{1,\mathrm{cap}} < 50(5+\sqrt{35})$. In this case, both eigenvalues of $\bar{x}_3$ are negative, which makes it a stable node. $\bar{x}_2$ is still a saddle point, stable in x_1-direction and unstable in x_2-direction. Still, all initial values converge to equilibrium point $\bar{x}_3$, but the difference with Figure 6d is that the predators do not die out.

Another observation worth investigating is that Figure 6b might show a limit cycle; undamped oscillations. The eigenvalues of the linearised system are $\lambda_{1,2} = -2 \cdot 10^{-7} \pm 0.1265\imath$, which indicate a very slow stable focus. It can be shown that the real part of $\lambda_{1,2}$ goes to 0 as $x_{1,\mathrm{cap}} \to \infty$, which corresponds with no grazing limit for the prey.

5.3 The Method

It was shown that a classification based on bifurcations results in a set of different behaviours and scenarios as a function of the uncertain parameters. This results in closed, dense sub-sets of the parameter space belonging to each scenario. The procedure that is used to classify this behaviour is summarized in [4] as follows:

1. Determine the equilibrium points as a function of the uncertain parameters and determine when they lay inside the boundaries of the states
2. Determine the eigenvalues of the linearised system at each equilibrium point as a function of the uncertain parameters
3. Find all sign changes in the eigenvalues, and when a switch between real and complex eigenvalues occurs
4. Determine stability of each equilibrium point based on Lyapunov's indirect method for each if possible

5. Combine the findings under 3. and 4. to form one list with scenarios
6. Compute separatrices numerically
7. Draw a phase portrait with separatrices
8. Determine the region of attraction for each stable equilibrium point and possible different trajectories that lead there (approach from below or approach from above)

The mathematical details and a more thorough treatment of the example can also be found in [4].

6 Validation of the Scenarios

In order to validate the scenarios found in Section 5, 100 runs were performed with random parameters and initial values as in Table 2. They were then classified in the three scenarios of Figure 6a, 6c and 6d.

In Figure 8, it can clearly be seen that the non-oscillatory scenarios differ a lot from the oscillatory scenario. Also, only six cases of the scenario is Figure 6c are present, which makes it easy to overlook in multi-run and clustering approaches.

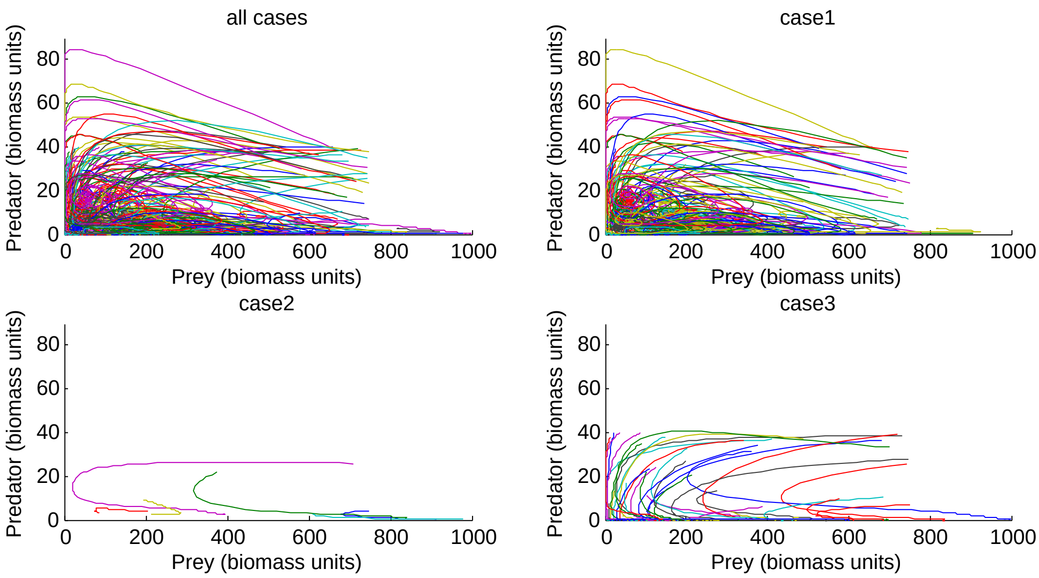

Figure 8: 100 runs with random parameters, predator vs. prey, sorted per scenario (forward time is counter clockwise)

The time-plots in Figure 9 show that in each scenario the time factor is not leading for classification. The proposed classification approach classifies behaviour based on similarity,

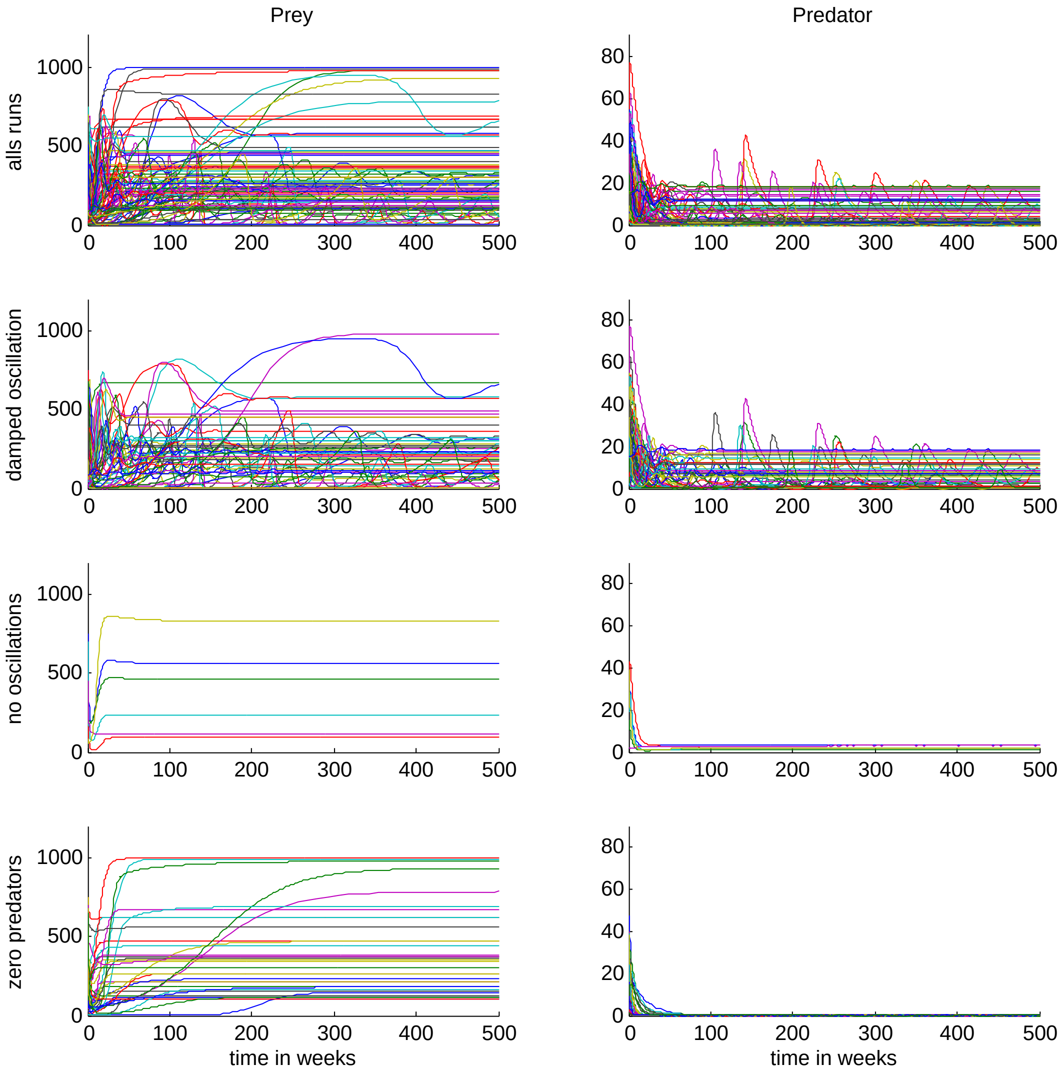

Figure 9: 100 runs with random parameters, time plots, sorted per scenario

not on minimal difference. Scaling and translation occurs a lot within each scenario, but they still behaviour according to the same pattern. Validation has thus shown that the proposed formal classification method can indeed classify behaviour analytically.

7 Conclusion and Discussion

This study treats formal behaviour classification of deeply uncertain non-linear systems in the context of System Dynamics (SD). The objective of this study was to develop a more insightful method to classify model behaviour for exploratory modelling.

A new approach to exploring a system is through formal analysis. In a phase portrait, the development over time of the system can be visualized for all initial values within a certain domain, for a fixed parameter set. Here, separatrices define boarders, separating different behaviours in a phase portrait.

Bifurcations are changes in the equilibrium points or periodic orbits, or their stability properties. These changes are induced by varying the uncertain parameters. As such, bifurcations can be seen as the boarders of the behavioural classes, because if they occur, an equilibrium point or its stability has changed. That makes the behaviour differ from the behavioural class under consideration. The conditions on the uncertain parameters that are found are the boundaries in the uncertainty space belonging to the boundaries of the behavioural classes.

No literature has been found of the application of this framework in more than two dimensions. It is recommended that further investigation into the applicability of the framework of behavioural regions on higher dimensions, with more stocks. Scaling up the method to more stocks and more uncertainties will only be feasible up to a certain level. It should be investigated where that boundary lies, with the currently available computing power. Also, it should be kept in mind that formal analysis before, after or in simultaneous with sampling and clustering could be even more accurate, insightful, or computationally efficient.

Another improvement would be to expand the approach to specifically search for all bifurcations, as they form the boundaries of the behavioural classes. This would enable the method to perform a full classification procedure and not require any other input then the uncertainties.

In general, formal analysis results in well-defined behavioural classes and class boundaries, also in the uncertainty space. That alone makes it worthwhile to further investigate the opportunities that formal analysis offers for behaviour classification under deep uncertainty, to provide modellers and policy makers with a complete insight into the possible scenarios to make conscious decisions for integral improvement.

References

[1] J. H. Kwakkel and E. Pruyt, "Exploratory modeling and analysis, an approach for model-based foresight under deep uncertainty," *Technological Forecasting and Social Change*, vol. 80, no. 3, pp. 419 – 431, 2013. Future-Oriented Technology Analysis.

[2] J. H. Kwakkel and E. Pruyt, "Using system dynamics for grand challenges: The esdma approach," *Systems Research and Behavioral Science*, 2013.

[3] S. Bankes, "Exploratory modeling for policy analysis," *Operations Research*, vol. 41, no. 3, pp. 435–449, 1993.

[4] J. Kuipers, "Classifying behaviour in uncertain non-linear systems."

[5] H. Bossel, *System Zoo 2 Simulation Models.* Books on Demand GmbH, Norderstedt, Germany, 2007.

[6] E. Pruyt, "System dynamics and uncertainty." r2v14, December 2013.

[7] C. van Daalen, E. Pruyt, W. A. H. Thissen, and H. W. G. Phaff, *Continuous Systems Models II.* Faculty of Technology, Policy and Management, Delft University of Technology, 2009.

[8] G. P. Richardson, "The core of system dynamics," *Encyclopedia of complexity and Systems Science*, 2008.

[9] G. P. Richardson, "Reflections on the foundations of system dynamics," *System Dynamics Review*, vol. 27, no. 3, pp. 219–243, 2011.

[10] G. Yücel and C. M. Chiong Meza, "Studying transition dynamics via focusing on underlying feedback interactions," *Computational and Mathematical Organization Theory*, vol. 14, no. 4, pp. 320–349, 2008.

[11] E. Pruyt, J. H. Kwakkel, and C. Hamarat, "Doing more with models: Illustration of a sd approach," in *Conference Proceedings of the 31st International Conference of the System Dynamics Society*, System Dynamics Society, 2013.

[12] C. Hamarat, J. H. Kwakkel, and E. Pruyt, "Adaptive robust design under deep uncertainty," *Technological Forecasting and Social Change*, vol. 80, no. 3, pp. 408 – 418, 2013. Future-Oriented Technology Analysis.

[13] G. Yücel and Y. Barlas, "Automated parameter specification in dynamic feedback models based on behavior pattern features," *System Dynamics Review*, vol. 27, no. 2, pp. 195–215, 2011.

[14] J. H. Kwakkel, W. L. Auping, and E. Pruyt, "Dynamic scenario discovery under deep uncertainty: The future of copper," *Technological Forecasting and Social Change*, vol. 80, no. 4, pp. 789 – 800, 2013. Scenario Method: Current developments in theory and practice.

[15] H. K. Khalil, *Nonlinear Systems.* Prentice Hall, Upper Saddle River, New Jersey 07458, third edition ed., 2002.

[16] E. M. Izhikevich, "Equilibrium," *Scholarpedia*, vol. 2, no. 10, p. 2014, 2007.

[17] J. Guckenheimer, "Bifurcation," *Scholarpedia*, vol. 2, no. 6, p. 1517, 2007.

[18] M. Brittenham, "A quick guide to sketching phase planes," 2003. Math 221 - Spring 2003.

[19] M. Brittenham, "A quick guide to sketching direction fields," 2009. Math 221 - Section 5 - Fall 2009.

[20] "Separatrix," December 2013. Encyclopedia of Mathematics.

[21] E. W. Weisstein, "Separatrix." From MathWorld–A Wolfram Web Resource.

[22] B. Ermentrout, "Nullclines and phaseplanes," September 2002.

A Phase Portraits

Khalil [15, p. 33-35] and Brittenham [18, 19] separately treat phase portraits by means of an example. A two-dimensional non-linear differential equation of the form

$$\dot{x}_1 = f_1(x), \quad \text{and} \quad \dot{x}_2 = f_2(x)$$

defines the derivative of the state for each x within a certain domain. The (unique) solution to this equation, denoted by $x(t) = [x_1(t),\ x_2(t)]^T$, starting in a given $x(0) = x_0$, is a curve in the $x_1 - x_2$-plane. This plane is also called the state plane or phase plane. The two dimensional function $f(x)$ defines the tangent vector $\dot{x} = [\dot{x}_1(t),\ \dot{x}_2(t)]^T$ to the curve $x(t)$. Therefore, $f(x)$ is the vector field on the state plane; it gives the direction as a vector $f(x)$ for every point x. This vector field can be visualized by gridding the state plane and plot the direction of $f(x)$ at every grid point, thus obtaining a vector field diagram. The length of an arrow is proportional to the magnitude of the derivative at that point $\sqrt{f(x)^T f(x)}$.

The family of all trajectories along the vector field is called the phase portrait of the differential equation. A phase portrait is usually visualized by plotting a couple of trajectories nicely positioned around the equilibrium points. When visualizing phase portraits, the goal is to get a grasp of the shape of the family of all trajectories.

Because of the fact that the actual solution $x(t)$ cannot be retrieved from a phase portrait. Therefore, the data in a phase portrait is qualitative instead of the quantitative data that would represent a solution over time.

B Separatrix

To guide in the interpretation of phase portraits, some particularly insightful solutions $x(t)$ are sought. The separatrix is a special solution that has the property to (locally) separate the state space in regions. Once a system is in one of those regions, it cannot get to the other region any more. Later, this will help in distinguishing different modes of behaviour.

The Encyclopedia of Mathematics, Weisstein and Ermentrout all use the example of a saddle equilibrium in two dimensions to introduce the concept [20, 21, 22]. As can be found in [15], an equilibrium point $\bar{x}$ is a saddle if the linearisation has two real eigenvalues of different sign, λ^+ and λ^- . Such vector field has two invariant curves through the equilibrium point. These trajectories are called separatrices of the saddle.

A distinction between the separatrices of a saddle point $\bar{x}$ can be made in a stable and an unstable manifold [20]. On the separatrix in the direction of the eigenvector v_{λ^-} belonging to the negative eigenvalue λ^- of the linearisation , $x(t) \rightarrow \bar{x}$ as $t \rightarrow \infty$. This is referred to as the stable separatrix, and can be found by solving the non-linear differential equations for $x_0 = \bar{x} \pm \varepsilon v_{\lambda^-}$. Here, ε is an arbitrary small, positive number. Conversely, on the unstable separatrix in the direction of the eigenvector v_{λ^+} associated with the positive eigenvalue λ^+ of the linearisation, $x(t) \rightarrow \bar{x}$ as $t \rightarrow -\infty$. The trajectories belonging to the unstable separatrix are found by solving the system with $x_0 = \bar{x} \pm \varepsilon v_{\lambda^+}$. Here, ε_i is an arbitrary small, positive weight of the contribution of eigenvector v_λ.

Sometimes the term separatrix is used for the stable and unstable invariant manifold of hyperbolic equilibrium points in higher dimensions as well [20]. This implies that, the manifolds are not necessarily a curve any more, but could as well be planes or higher dimensional manifolds. This complicates working with separatrices in higher dimensions, because of the fact that solutions to the non-linear differential equation they belong to are seldom analytic. This means that the family of all trajectories has to be approximated by solving the system with, possibly, a very large number of initial states that are linear combinations of the eigenvectors locally spanning the manifold: $x_0 = \varepsilon_1 v_{\lambda_1^-} + \ldots + \varepsilon_p v_{\lambda_p^-}$ for p stable eigenvalues and $x_0 = \varepsilon_1 v_{\lambda_1^+} + \ldots + \varepsilon_p v_{\lambda_p^+}$ for p unstable eigenvalues. This make the separatrix less insightful in higher dimensions.